J. Anat. (1997) **190**, pp. 589–600, with 22 figures Printed in Great Britain

Fine structure of the cap enameloid and of the dental epithelial cells during enameloid mineralisation and early maturation stages in the tilapia, a teleost

ICHIRO SASAGAWA

Department of Anatomy, The Nippon Dental University, Niigata, Japan

(*Accepted 2 January 1997*)

ABSTRACT

Morphological features of the cap enameloid and dental epithelial cells were investigated by light and transmission electron microscopy during the various stages of enameloid mineralisation and early maturation in the tilapia. The pattern of mineralisation along collagen fibrils in the enameloid differed from that in the dentine. Many matrix vesicles were found in the predentine and in the enameloid, suggesting that they may be involved in the initial mineralisation in both regions. Most of the organic matrix disappeared from the cap enameloid during mineralisation and maturation. The disappearance of the organic matrix could be divided into 2 stages. Initially a fine network-like matrix, which probably consisted of glycosaminoglycans and extended between collagen fibrils, began to disappear. At the same time, fine crystallites and electron-dense, fine granular material covered the collagen fibrils as mineralisation of the enameloid began. In the second stage, the maturation of the enameloid, the collagen fibrils degenerated completely and disappeared from the cap enameloid, being replaced by large numbers of large crystals. At the mineralisation stage, the numbers of lysosomal bodies tended to increase in the inner dental epithelial (IDE) cells, which contained a well developed Golgi apparatus and rough endoplasmic reticulum (rER). At the early stage of maturation, a ruffled border was noted at the distal ends of the IDE cells, which contained many mitochondria and lysosomal bodies, but less rER. These features suggest that the cells actively absorb the organic matrix, which includes collagen fibrils, in the cap enameloid. The outer dental epithelial (ODE) cells were translucent cells that contained well developed labyrinthine canalicular spaces from the onset of the mineralisation stage to the middle stage of maturation. The IDE and ODE cells were clearly involved in the mineralisation of the cap enameloid at the mineralisation and maturation stages.

Key words: Mineralisation; collagen fibrils; enameloid; tilapia; tooth development.

INTRODUCTION

The relationship between the degeneration of the organic matrix, including collagen fibrils, and the growth of the crystals in the enameloid of teleosts is an interesting subject in the field of biomineralisation research. The initial mineralisation in the tooth germs in teleosts begins at the boundary between the cap enameloid, which contains abundant collagen fibrils, and the predentine (Isokawa et al. 1970; Shellis & Miles, 1974, 1976; Yamashita & Ichijo, 1983; Sasagawa, 1984, 1988). Large numbers of matrix vesicles (MVs), which often enclose needle-like crystallites, are found in the enameloid matrix, in particular near the boundary, and this observation suggests that MVs may be actively involved in the initial mineralisation (Sasagawa, 1988). Mineralisation spreads centrifugally from the site of initial mineralisation to the enameloid and it spreads centripetally to the dentine. In the cap enameloid, fine crystals are deposited along the collagen fibrils and the deposition of crystals progresses to the surface of the enameloid during mineralisation of the enameloid (Shellis & Miles, 1974; Prostak & Skobe, 1986; Sasagawa, 1988). When the enameloid matures, however, the collagen fibrils degenerate and are

Correspondence to Dr Ichiro Sasagawa, Department of Anatomy, The Nippon Dental University, 1–8 Hamaura-cho, Niigata 951, Japan.

replaced by large enameloid crystals. The arrangement of the collagen fibrils can be deduced from the pattern of crystals in the mature enameloid that lacks collagen fibres (Schmidt, 1971; Shellis & Miles, 1974; Prostak & Skobe, 1986). The highly mineralised, mature cap enameloid corresponds to the tooth enamel in mammals. However, there have been only a few morphological studies of mineralisation in the enameloid (Shellis & Miles, 1976; Prostak & Skobe, 1986). It seems likely that dental epithelial cells play an important role during maturation in the enameloid. The inner dental epithelial (IDE) cells, with a ruffled border at the distal end of each cell, and the outer dental epithelial (ODE) cells, in which extensive canalicular spaces develop, are thought to remove the organic matrix from the enameloid and to transport inorganic ions, such as calcium ions, to the enameloid. It has also been postulated that the epithelial cells secrete organic materials, such as enzymes, to the developing enameloid (Shellis & Miles, 1974; Sasagawa, 1984, 1992; Prostak & Skobe, 1986). Results of immunohistochemical (Herold et al. 1989) and ultrastructural (Sasagawa & Ferguson, 1990) studies have indicated the probable existence of enamelines in the cap enameloid of teleosts, but more recent immunohistochemical studies have provided evidence that neither amelogenines nor enamelines are present in the enameloid (Prostak et al. 1991; Ishiyama et al. 1994). Accumulation of iron at the maturation stage is an unusual feature of the IDE cells in tilapia, and the details of this accumulation have been reported by Sasagawa (1992, 1993). It is also known that the IDE and ODE cells are involved in the transport of iron during the maturation stage. However, little information is available about the morphological features of the dental epithelial cells during the various stages of enameloid mineralisation and early maturation. The morphological relationship between the degeneration of collagen fibrils and the early stages of mineralisation in enameloid is still unclear, as is the contribution of the epithelial cells to the mineralisation of the enameloid. The aim of the present study was to characterise the ultrastructural changes associated with mineralisation in the cap enameloid and the dental epithelial cells during the various stages of enameloid mineralisation and early maturation.

MATERIALS AND METHODS

Five artificially bred adult tilapias, *Oreochromis niloticus*, Cichlidae (total length 35–37 cm), were obtained from Hokuetsu Mizugiken Inc., Niigata, Japan for this study.

After decapitation, pharyngeal teeth containing tooth germs were dissected out and fixed in 10% buffered formalin (cacodylate buffer, pH 7.4) for 3 d. The specimens were demineralised by incubation in 5% formic acid for 2 wk. After dehydration and embedding in paraffin wax, serial sections were prepared. These sections were stained with haematoxylin–eosin (H–E), azan, elastic–van Gieson and periodic acid-Schiff (PAS) plus Alcian blue and examined under a light microscope. Some sections were stained with PAS–Alcian blue after pretreatment with human saliva containing salivary amylases for 60 min at 37 °C.

Other regions of the pharynx were placed in Karnovsky's fixative (cacodylate buffer, pH 7.4) overnight at room temperature. Most of the specimens were then fixed in a 1% solution of osmium tetroxide in cacodylate buffer, and some of them were demineralised in a 2.5% solution of disodium EDTA for 3 wk before postfixation. After dehydration, these specimens were embedded in Araldite–Epon resin. Some specimens were embedded directly in glycol methacrylate (GMA) resin after prefixation and dehydration. Semithin sections were cut with glass knives, stained with toluidine blue and examined under the light microscope. Ultrathin sections were cut with glass or diamond knives. They were usually stained with uranyl acetate and lead citrate (U-Pb) and then examined with a transmission electron microscope (TEM; Hitachi H-500 or JEOL JEM-1200EX). To gain information on crystals, selected-area electron diffraction (SAED) patterns were sometimes obtained from nondemineralised sections by TEM.

RESULTS

Enameloid mineralisation stage

Light microscopy

A dentine matrix was apparent on the basal side of the fully formed cap enameloid matrix, and mineralisation started at the boundary between the enameloid and the dentine. The mineralised dentine and unmineralised predentine were clearly distinguishable at this stage. In the enameloid, mineralisation advanced from the boundary between the enameloid and the dentine to the apex of the enameloid (Fig. 1).

Capillaries, together with ODE cells, penetrated the layer of IDE cells in some places. As a result, the outlines of the layers of dental epithelial cells near the

apex appeared convoluted. The ODE cells developed into large and more translucent cells, forming a layer of simple cuboidal epithelial cells. The IDE cells became slightly more translucent and longer, and a nucleus was usually observed in the proximal region of each cell (Fig. 1).

This stage might be rather brief, since tooth germs were rarely found, and it can be considered to correspond to the transitional stage between formation of the enameloid matrix and maturation of the enameloid.

Transmission electron microscopy

In the predentine, collagen fibrils that were about 30 nm in thickness, resembling those in the enameloid matrix, were arranged in intricate patterns, but did not form thick bundles. Many matrix vesicles (MVs) of 30–80 nm in diameter, many odontoblast processes and a fine granular matrix were visible among the fibrils. The mineralisation front was conspicuous and fairly straight, with occasional small aggregations of crystallites at the front (Fig. 2).

In the enameloid, deposition of crystallites, which progressed along collagen fibrils, extended towards the apex. The pattern of mineralisation in the enameloid was clearly different from that in the dentine (compare Figs 2 and 3). In the enameloid, in contrast to the dentine, many crystallite-free collagen fibrils remained among the mineralised fibrils on which crystallites had accumulated. A clear mineralisation front, of the type seen in the dentine, was not visible in the enameloid, and deposition of crystallites in the enameloid seemed to progress along collagen fibrils exclusively. Fine aggregations composed of crystallites were seldom found in the enameloid. Some electron-dense particles were usually observed on crystallite-free collagen fibrils that were near mineralised collagen fibrils. At sites at which needle-like crystallites of $\sim$2–4 nm in thickness accumulated along collagen fibrils, electron-dense finely granular materials were found, and the periodic stripes of collagen fibrils were scarcely visible (Fig. 3). Several MVs that did not contain any crystallites were often seen among the mineralised collagen fibrils (Fig. 3, inset), and odontoblast processes were observed in the inner layer of the enameloid.

When mineralisation had reached the apex of the enameloid (Figs 1, 4), the construction of the enameloid matrix in the outer layer changed. In this outer layer, the bundles of the collagen fibrils became looser, with wide spaces among the fibrils, and individual collagen fibrils began to meander through the demineralised regions (Fig. 5). The fine flocculent material among the collagen fibrils disappeared in the outer layer. However, the thickness of the collagen fibrils remained unchanged and their periodic stripes were visible in demineralised sections (Fig. 5, inset). There were limited numbers of defined MVs among the collagen fibrils but only a few odontoblast processes. At the sites of mineralised collagen fibrils, electron-dense finely granular materials masked the fibril bundles. However, the periodic stripes of the collagen fibrils were often still visible after treatment with the solution of disodium EDTA (Fig. 6).

In the cytoplasm of the extended IDE cells, the rough endoplasmic reticulum (rER) was well developed, with many mitochondria in the proximal region of each cell (Fig. 7). An extensive Golgi apparatus occupied the distal cytoplasm of each cell. Large granules containing electron-dense material and with irregular profiles were usually seen near the Golgi apparatus (Fig. 7, inset). Round lysosomal bodies were scattered in the cytoplasm. Expanded intercellular spaces were visible among the IDE cells. There were several projections from the lateral cell membrane into these spaces. The IDE cells made contact, via desmosomes and gap-like junctions, at such projections. Junctional complexes were apparently present in the distal regions of the IDE cells. The distal cell membranes of the IDE cells were smooth, without obvious infoldings (Fig. 7). A basal lamina was visible, but disappeared during mineralisation at the outermost layer.

The ODE cells contained labyrinthine canalicular spaces that occupied most of the cytoplasm (Figs 8, 9). Small numbers of mitochondria, short stretches of rER, filaments, granules that contained electron-dense materials, ribosomes, vacuoles and vesicles were found in the narrow spaces between the canaliculi. A large nucleus was situated near the centre of each ODE cell (Fig. 9). A less extensive Golgi apparatus was located near the nucleus. There were long gap-like junctions and desmosomes at the nonconvoluted interface between the IDE and the ODE cells.

Maturation of the enameloid

Light microscopy

After mineralisation had reached the apex, further mineralisation occurred in the outermost layer of the enameloid, spreading eventually through the entire enameloid (Fig. 10). At the middle stage of enameloid maturation, only a small amount of the organic matrix was retained in the enameloid (Figs 11, 12).

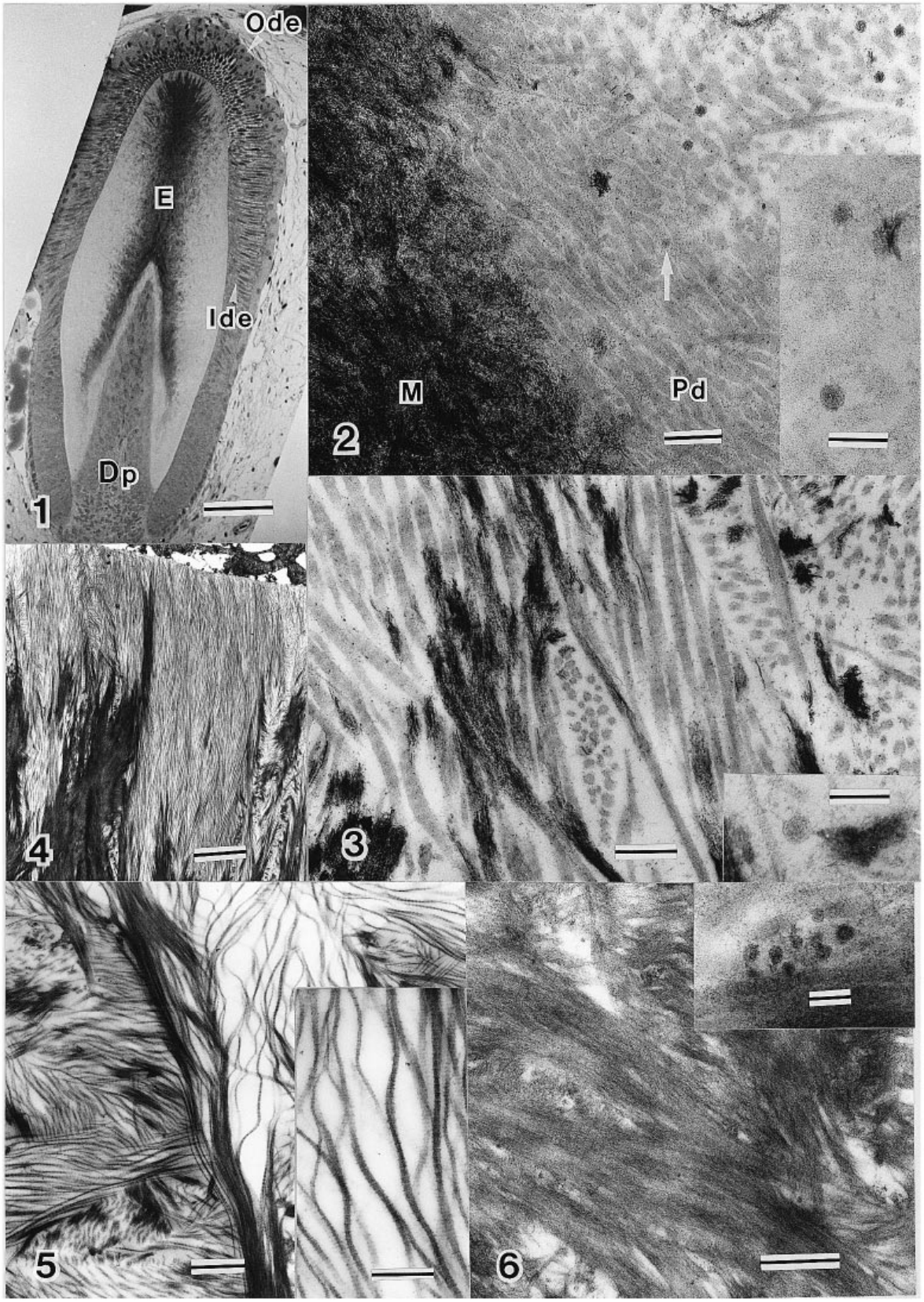

Figures 1 and 10–12 are light micrographs; Figures 2–9 and 13–22 are transmission electron micrographs contrasted with uranyl acetate and lead citrate.

Fig. 1. Tooth germ at the later stage of enameloid mineralisation. The mineralisation has reached the apical part of the enameloid. The mineralised area has been stained more deeply with toluidine blue in a demineralised section as a consequence of differences in the nature of the organic matrix, as for mammalian dentine (Ten Cate, 1989). Dp, dental papilla; E, mineralised enameloid; Ide, inner dental epithelium;

The layer of IDE cells was uneven as a result of the deep penetration of the capillaries into the dental epithelial cell layer (Figs 11, 12). The nuclei were located in the proximal regions of the tall IDE cells. The ODE cells that formed a layer of simple cuboidal epithelial cells around the capillaries had almost spherical nuclei, and they were translucent and slightly eosinophilic. The ODE cells were stained more strongly by PAS–Alcian blue than were the IDE cells (Fig. 12).

The stage of enameloid maturation might be relatively long since several tooth germs at this stage were frequently found in sections examined by light microscopy.

Transmission electron microscopy

Enameloid at the early stage. In the outer layer of the enameloid, slender crystallites 6–7 nm thick (thicker than those at the enameloid mineralisation stage) were visible in large numbers on electron micrographs. SAED patterns from this layer indicated that it contained apatite (Fig. 13). Many round and elliptical electron-dense materials 12–40 nm in diameter were observed among the crystallites (Fig. 13, inset). In some cases, the electron-dense materials appeared to combine with the slender crystallites, suggesting that the materials might have been part of the crystallites, which were plate-like in shape. In the inner layer of the enameloid, the long axes of the crystallites tended to be oriented in the direction of the long axes of the collagen fibrils, although most of the collagen fibrils in the enameloid had disappeared, apart from a few fragments of fibrils with the typical cross-banding pattern (Fig. 14). The basal lamina was hardly visible at the early stage of enameloid maturation.

Enameloid at the middle stage. In nondemineralised sections, the enameloid was mostly occupied by large numbers of crystals at the middle stage of mineralisation (Fig. 15). Slender crystals, which were 10–15 nm thick and often contained an electron-lucent line in the centre, were usually found in the inner layer (Fig. 16). In the outer layer, by contrast, prismatic crystals 20–30 nm in thickness were abundant (Fig. 17). In demineralised sections, most enameloid constituents, with the exception of some microfibrils and tubular structures, were dissolved by the solution of disodium EDTA. No collagen fibrils were found at this stage. At the boundary between the enameloid and the dentine, the thick collagen fibrils with defined cross-banding in the dentine changed into fine microfibrils that formed a scattered network. In the inner layer of the enameloid, an organic matrix was observed, consisting of many microfibrils which formed a network (Fig. 18). Numerous fine tubular structures, each $\sim$ 16 nm thick and 250 nm long, were found in the outer layer close to the IDE cells in the cervical region (Fig. 19). The tubular structures decreased in number in the inner layer. Conversely, many microfibrils were visible in the inner layer, but few in the outer layer of the cervical portion of the cap enameloid. Neither tubular structures nor microfibrils were visible in the apical enameloid space.

Dental epithelial cells. Infoldings of the cell membrane were seen at the distal ends of IDE cells at the early stage (Fig. 20). The infoldings became a well developed ruffled border at the middle stage. This border appeared to consist of finger-like projections of the distal cell membrane. Cisternae containing electron-dense flocculent and/or fine granular ma-

---

Ode, outer dental epithelium. Sections were demineralised in a 2.5% solution of disodium EDTA and stained with toluidine blue. Bar, 100 μm.

Fig. 2. Mineralisation front in the dentine at the enameloid mineralisation stage. The mineralisation front is visible as a defined line, and fine granular materials are abundant along the front. Arrow shows a matrix vesicle covered by fine granular material. M, mineralised dentine; Pd, predentine. Not demineralised. Bar, 200 nm. Inset: enlarged view of matrix vesicles. Nondemineralised, U-Pb. Bar, 100 nm.

Fig. 3. Mineralisation in the enameloid at the enameloid mineralisation stage. The pattern of mineralisation differs from that in the dentine, as shown in Figure 2. Unmineralised collagen fibrils can be seen among the mineralised fibrils. Needle-like crystallites are visible close to the collagen fibrils. Their long axes are almost parallel to those of the collagen fibrils. Nondemineralised. Bar, 200 nm. Inset: round matrix vesicle between mineralised collagen fibrils. Not demineralised. Bar, 100 nm.

Fig. 4. Apical area of the enameloid at the later stage of enameloid mineralisation. Electron-dense regions represent the mineralised enameloid matrix that has been stained intensely by U-Pb. Demineralised, Bar, 2 μm.

Fig. 5. Enameloid matrix at the later enameloid mineralisation stage. Collagen fibrils are less closely packed and the spaces between the collagen fibrils appear to be wide and empty. Demineralised, U-Pb. Bar, 1 μm. Inset: enlarged view of the collagen fibrils in the outer layer. While the periodic stripes on the collagen fibrils are still visible, the fibrils have started to meander and the flocculent material between the fibrils has disappeared. Demineralised. Bar, 500 nm.

Fig. 6. Enlarged view of the mineralised enameloid area after demineralisation with disodium EDTA. Fine electron-dense granular material masks the collagen fibrils, although the striations on the collagen fibrils can still be seen. U-Pb. Bar, 500 nm. Inset: MVs in the mineralised enameloid area. Demineralised. Bar, 100 nm.

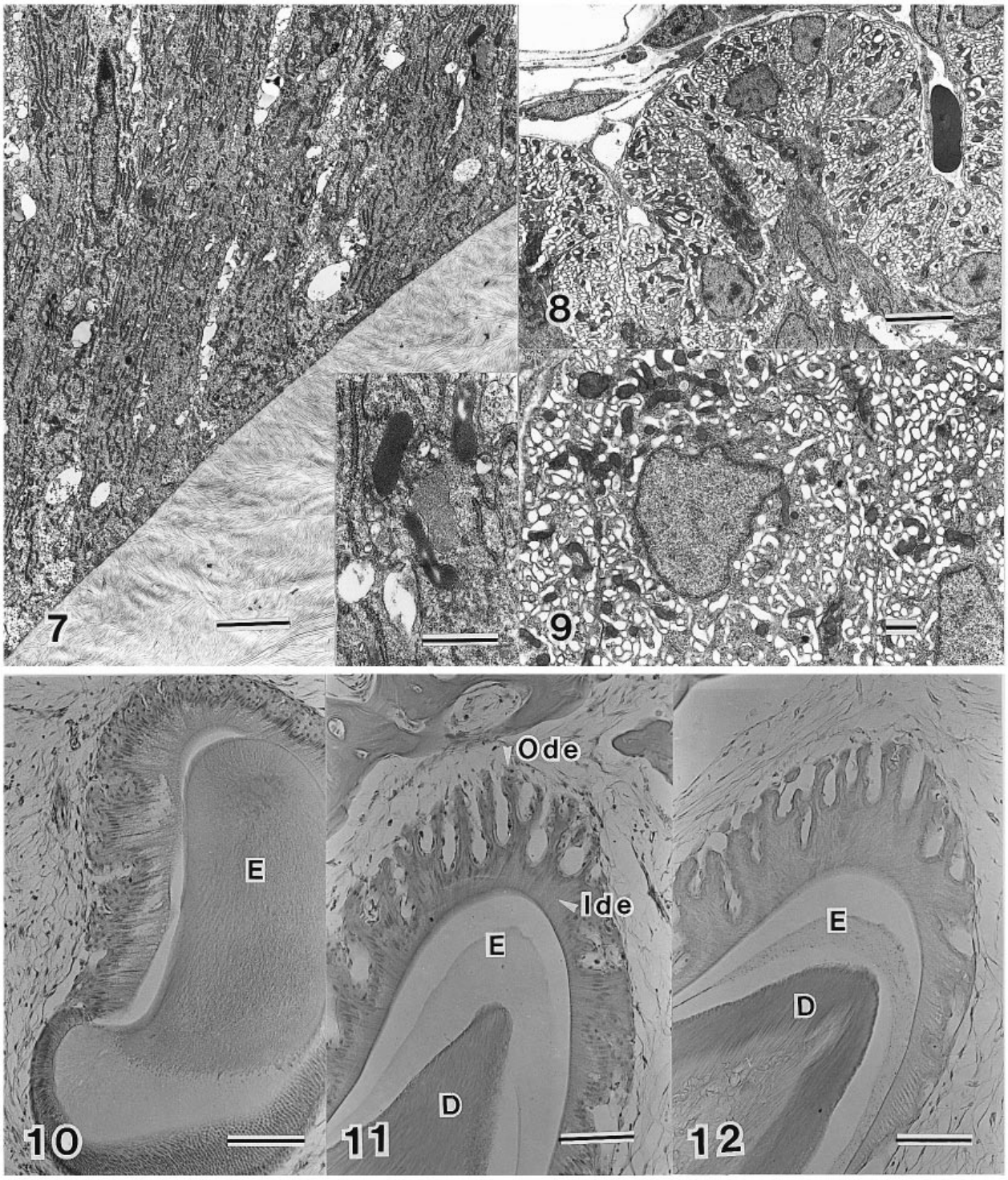

Fig. 7. Distal portion of IDE cells at the enameloid mineralisation stage. Much rER and many large lysosomal bodies are visible in the cytoplasm. Demineralised. U-Pb. Bar, 3 μm. Inset: several large granules containing electron-dense material or electron-lucent cores. Demineralised. Bar, 100 nm.

Fig. 8. A layer of ODE cells interrupted by penetrating capillaries at the enameloid mineralisation stage. Demineralised. U-Pb. Bar, 5 μm.

Fig. 9. Enlarged view of the ODE cells. Most of the cytoplasm is occupied by canalicular spaces. Demineralised. Bar, 1 μm.

Fig. 10. Tooth germ at the early stage of enameloid maturation. Mineralisation has spread through most of the enameloid (E) but a coarse fibrous structure that has been stained by haematoxylin is visible in the enameloid. Demineralised with 5% formic acid, stained with H-E. Bar, 100 μm.

Fig. 11. Apical part of a tooth germ at the middle stage of enameloid maturation. Little of the organic matrix remains in the enameloid space (E) after demineralisation with formic acid. Many capillaries have penetrated deeply into the dental epithelial cell layer. D, dentine; Ide, inner dental epithelium; Ode, outer dental epithelium. H-E. Bar, 100 μm.

terial were visible at the proximal ends of the infoldings of the distal cell membranes (Figs 20, 21). There were many mitochondria, primary lysosomal bodies and multivesicular bodies in the distal cytoplasm near the ruffled borders (Figs 20, 21). A few mitochondria, short stretches of rER, smooth endoplasmic reticulum (sER), electron-dense bodies and ribosomes were observed around the Golgi apparatus that was located in the central part of the cytoplasm (Fig. 22). The distal portions of the IDE cells adhered to one another (Fig. 21). Many projections from lateral cell membranes and wide intercellular spaces between IDE cells were seen from the central to the proximal region of these cells. Desmosomes and short gap-like junctions were usually found at the sites on the projections at which the IDE cells adhered to one another. Many electron-dense particles, which were round, 5.5 nm in diameter, and probably ferritin (Sasagawa, 1992, 1993), were scattered in the cytoplasm of the IDE cells, as well as several large granules that contained electron-dense fine particles at the middle stage. In the ODE cells, the cytoplasm was almost completely filled with well developed, labyrinthine canalicular spaces (Fig. 22). The fine structure of the ODE cells was nearly the same as that at the mineralisation stage. An orderly arrangement of desmosomes and gap-like junctions was characteristic at the boundary between the IDE and ODE cells (Fig. 22, inset). Few electron-dense particles 5.5 nm in diameter were observed in the ODE cells.

DISCUSSION

In the tilapia, the pattern of mineralisation of the enameloid was different from that of the dentine at the mineralisation stage, while both the enameloid and the dentine contained large numbers of collagen fibrils. A clear mineralisation front was visible in the dentine but not in the enameloid. In the enameloid, a convoluted pattern of mineralised and unmineralised collagen fibrils was observed during the mineralisation stage. It has been reported that the complex pattern of mineralisation in the enameloid is associated with a change in the arrangement of collagen fibrils (Sasagawa, 1988). It also seems likely that the participation of odontoblasts and dental epithelial cells during mineralisation is one reason for the difference in the pattern of mineralisation between the dentine and the enameloid at the mineralisation stage. It is generally thought that mineralisation in the dentine is closely regulated by odontoblasts (Ten Cate, 1989; Linde & Goldberg, 1993). In the enameloid, by contrast, odontoblast processes seem to decrease in number after formation of the matrix. Mineralised dentine is situated between the enameloid and the odontoblasts at the mineralisation stage. Therefore, the difference could indicate that mineralisation in the enameloid at the mineralisation stage is controlled to a lesser extent by odontoblasts, even if at least part of its organic matrix is produced by odontoblasts when the matrix is formed. The fibrous organic components in the enameloid are thought to be composed of ectodermal collagen and collagen fibrils formed by odontoblasts (Prostak et al. 1992; Sasagawa, 1995). It is also possible that the existence of ectodermal collagen in the enameloid is responsible for the distinctive pattern of mineralisation.

Many matrix vesicles (MVs) were observed in the predentine and in the organic matrix among the mineralised collagen fibrils in the enameloid. It seems likely that the MVs are involved in the initial mineralisation in both the dentine and the enameloid. Fibrous electron-dense material, which appeared to originate from MVs during dentinogenesis in the dog salmon, (*Oncorhynchus*, Sasagawa & Igarashi, 1985), was not found in the enameloid matrix of the tilapia.

Prior to the deposition of crystals at the mineralisation stage, the spaces between the collagen fibrils at the outer layer of the enameloid became clearly defined because the fine flocculent material that had formed a network around the collagen fibrils was no longer visible, and individual collagen fibrils meandered through this region. It seems probable that the material between the collagen fibrils degenerated before the disappearance of the collagen itself. It has been reported that sulphated glycoconjugates are located around the collagen fibrils in the developing cap enameloid and that they decrease markedly in number in the mature enameloid in bichirs (*Polypterus*), while in the knifejaws (*Hoplognathus*) chondroitin sulphate is still found in association with collagen fibrils as they are degraded (Kogaya, 1989, 1994). In tilapia, the enameloid matrix was stained by PAS–Alcian blue during formation of the enameloid matrix, a result that suggests that large amounts of glycosaminoglycans (GAGs) might be present in the matrix during this period (Sasagawa, 1995). Finely

Fig. 12. Apical part of a tooth germ stained with PAS–Alcian blue at the middle stage of enameloid maturation. Few PAS–positive particles are visible in the IDE cells. D, dentine; E, enameloid space. Bar, 100 μm.

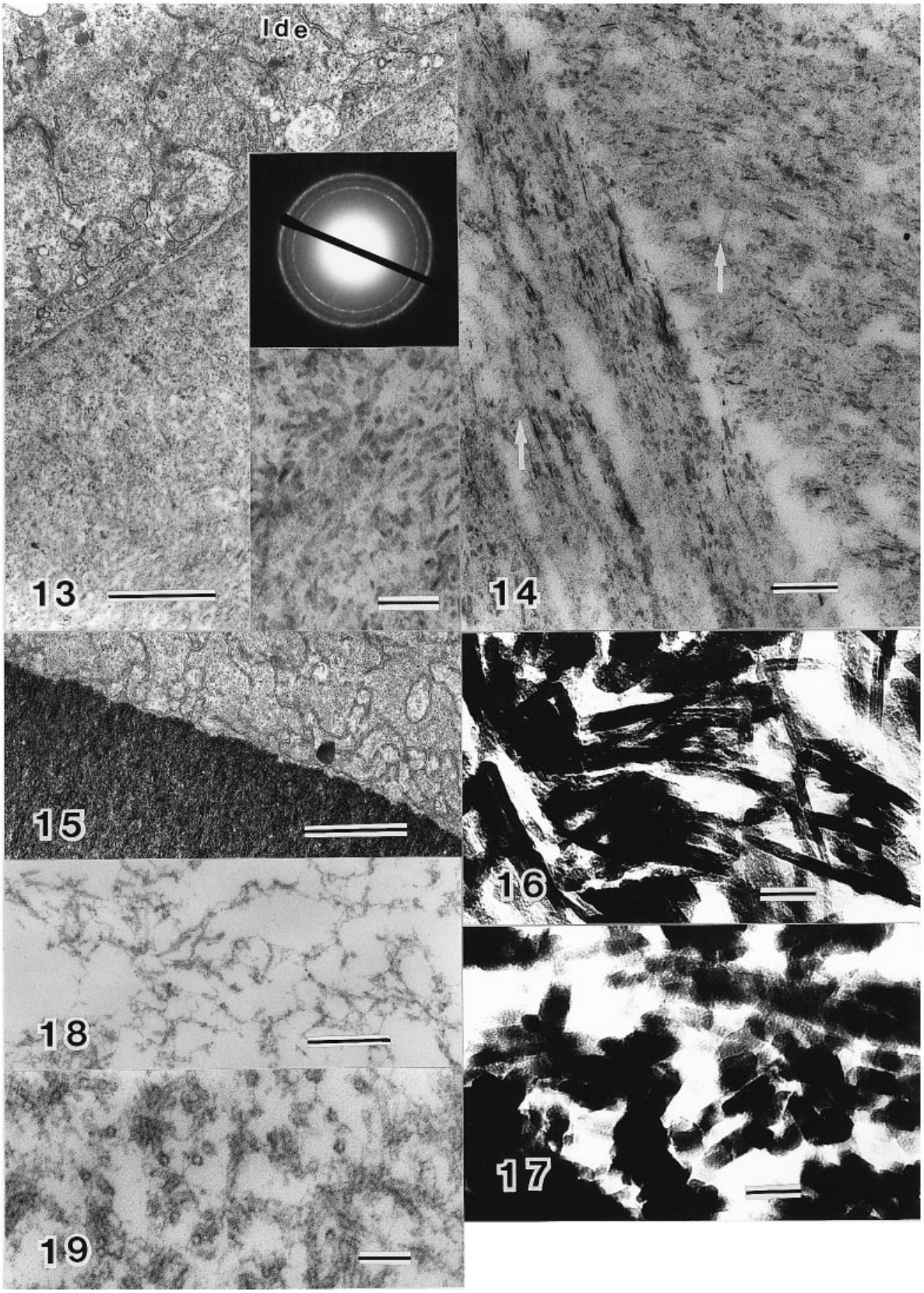

Fig. 13. Outer layer of enameloid at the early stage of enameloid maturation. Many crystallites are visible in the outermost layer of the enameloid. A basal lamina is hardly detectable at this stage. Ide, inner dental epithelium. Nondemineralised, U-Pb. Bar, 1 μm. Inset (upper): SAED pattern of apatite obtained from crystallites in the enameloid. Inset (lower): enlarged view of the outer layer of mineralised enameloid. Electron-dense material is visible around the crystallites. Ghost-like crystal structures that appear hollow are the result of partial demineralisation during staining with uranyl acetate. The mineralised portion appears to be covered with fine granular material and there are many irregularly shaped small granules of electron-dense material. Not demineralised. Bar, 100 nm.

textured material, thought to be GAGs and forming a network-like array between collagen fibrils, was actually found in the developing enameloid matrix (Sasagawa, 1995). It is possible, therefore, that GAGs that associate with the collagen fibrils in the cap enameloid when the enameloid matrix is formed might be digested and removed predominantly during the mineralisation stage. Such events would support the hypothesis that removal of materials that inhibit the progress of mineralisation leads to mineralisation from the boundary between the enameloid and the dentine to the surface of the enameloid (Sasagawa, 1988).

At the maturation stage, most of the organic matrix in the enameloid disappeared and the extent of mineralisation became greater in the enameloid. There is no question that collagen fibrils are absorbed and removed from the enameloid. The results obtained in the present study agree with the results of Shellis & Miles (1976) who reported that no collagen fibrils were present in the enameloid spaces at the maturation stage, with the exception of a few fragments that resembled microfibrils in sections that had been demineralised with disodium EDTA. Moreover, the collagen fibrils appeared to change into scattered microfibrils at the boundary between the enameloid and the dentine, and these microfibrils clearly originated from collagen. Kawasaki et al. (1987), Shimoda (1989) and Prostak et al. (1992) detected proteolytic activity, which might be involved in the digestion of collagen fibrils, in the enameloid, although collagenase has not been found in the enameloid at this time. The absorption and removal of collagen and other components of the organic matrix obviously provide the space required for growth of crystals in teleost enameloid during the maturation stage.

It is likely that the process of mineralisation in the cap enameloid and the removal of the organic matrix from the enameloid proceeds in 2 stages. First, the matrix, which includes GAGs, is removed from the spaces between the collagen fibrils at the mineralisation stage, and electron-dense materials cover the collagen fibrils, with the accumulation of slender crystallites along the fibrils. Secondly, the mineralised collagen fibrils degenerate in the enameloid and disappear from it during the maturation stage, when the crystals grow and the enameloid becomes hypermineralised.

Fine tubular structures of 16 nm in thickness have been observed in the outer layer of the enameloid during mineralisation of the enameloid in several teleosts (Ono, 1974; 15 nm thick, Kawasaki & Fearnhead, 1983; 20–40 nm thick, Yamashita & Ichijo, 1983). It has been postulated that these structures originate from the IDE cells and are actively involved in mineralisation of the enameloid (Yamashita & Ichijo, 1983). However, the region in which they are located is limited to the outer layer of the enameloid, and large numbers of tubular structures were still seen in the enameloid space in demineralised sections at the maturation stage. Some tubular structures 7–17 nm thick were observed between the electron-dense compartments, which had the same profiles as enameloid crystals and seemed to be crystal ghosts, in sections that had been demineralised with chromium sulphate (Sasagawa & Ferguson, 1990). It seems unlikely, therefore, that the tubular structures are important for the synthesis of large crystals in the enameloid. It is possible, however, that the tubular structures might be the remains of degenerated collagen fibrils in the enameloid.

The ODE cells had an unusual morphological feature from the beginning of the mineralisation stage to the middle of the maturation stage. Most of the cytoplasm of these cells was occupied by labyrinthine canalicular spaces. During this period, capillaries were close to the ODE cells. This organisation supports the hypothesis that the ODE cells might be involved in the active transport of inorganic ions (Garant, 1970) and, in particular, in the transport of fluoride (Prostak et al. 1993). It has been reported that ODE cells tend

Fig. 14. Enlarged view of the middle layer of the mineralised enameloid. Collagen fibrils are scarcely visible in this area, with the exception of a few tiny fragments (arrows). Nondemineralised, U-Pb. Bar, 200 nm.

Fig. 15. Outer layer of the mineralised enameloid and the distal portion of IDE cells at the middle stage of enameloid maturation. The enameloid contains large numbers of crystals. Not demineralised. Bar, 1 μm.

Fig. 16. Slender enameloid crystals in the inner layer. Embedded in GMA without postfixation in osmium tetroxide; not demineralised or stained. Bar, 50 nm.

Fig. 17. Prismatic enameloid crystals in the outer layer. Embedded in GMA without postfixation. Not demineralised or stained. Bar, 50 nm.

Fig. 18. Enlarged view of the residual organic matrix in the inner layer of the enameloid after demineralisation with disodium EDTA at the middle stage of enameloid maturation. A coarse network-like structure containing a number of tubular structures is visible. U-Pb. Bar, 500 nm.

Fig. 19. Enlarged view of tubular structures in the outer layer of the enameloid. The long axes of the tubular structures, which are ~ 16 nm thick, are oriented in various directions. Demineralised. Bar, 100 nm.

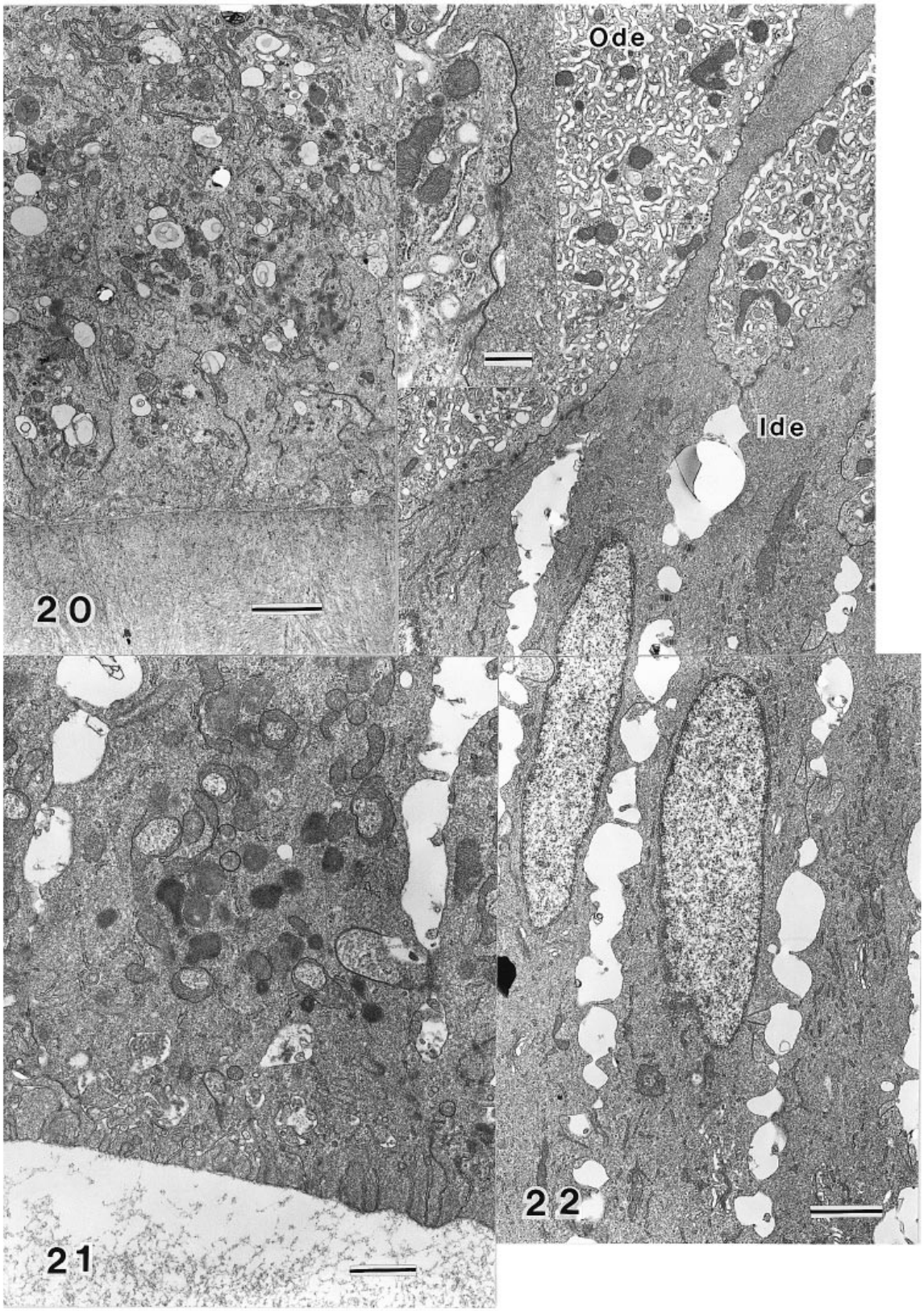

Fig. 20. Distal portions of IDE cells at the early stage of enameloid maturation. Infoldings of cell membranes are visible at the distal ends and several cisternae containing electron-dense material have formed at the proximal ends of the infoldings. Not demineralised, U-Pb. Bar, 2 μm.

Fig. 21. Distal portions of IDE cells at the middle stage of enameloid maturation. The infoldings of the distal cell membranes seem to form many projections, and coated vesicles and pinocytotic vesicles often make contact with the cisternae of the infoldings. Many mitochondria and lysosomal bodies can be seen in the distal cytoplasm near the ruffled border. Many adhesion sites that resemble junctional complexes are present in the distal regions. Demineralised. Bar, 1 μm.

to develop membrane-bounded spaces, for example, sER, vesicles and vacuoles, at the end of the enameloid matrix-formation stage (Sasagawa, 1995), and that the ODE cells contain increased numbers of tubular vacuoles when the IDE cells are associated with a matrix that contains small, finely packed enameloid crystals (Prostak & Skobe, 1986). The present study showed that the ODE cells were converted to cells that could actively transport inorganic ions prior to the maturation stage when the IDE cells had marked ruffled borders and collagen fibres had disappeared from the enameloid.

The arrangement of organelles in the IDE cells at the mineralisation stage was basically similar to that at the enameloid matrix-formation stage. The IDE cells still resembled secretory cells. However, while they contained no procollagen granules, they did contain many electron-dense granules that seemed to resemble lysosomal bodies. In the outermost layer of enameloid, facing the IDE cells, the fine flocculent material between collagen fibrils tended to disappear at an earlier time. Thus, probably, the absorptive function of the epithelial cells has a major influence on the outermost layer. Although marked ruffled borders were not apparent at the distal ends of IDE cells, we can assume that the IDE and ODE cells were actively involved in the digestion and removal of part of the organic matrix in the enameloid, supporting the hypothesis that the IDE cells secrete some enzyme, such as a protease, at the early stage of mineralisation (Prostak & Skobe, 1986).

The IDE cells with marked ruffled borders at their distal ends and the ODE cells with their abundant canaliculi can safely be assumed to be actively involved in the degeneration of the organic matrix and in its removal from the enameloid in several teleosts (Wakita, 1974; Shellis & Miles, 1976; Sasagawa, 1984; Prostak & Skobe, 1986). Cisternae containing electron-dense flocculent material have been observed at the proximal ends of the ruffled borders in several teleosts, and the electron-dense contents are thought to correspond to the digested material derived from the enameloid matrix and the basal lamina (Shellis & Miles, 1976; Prostak & Skobe, 1986). The many lysosomes and mitochondria that accumulate at the proximal portion of the well developed ruffled borders in the IDE cells are probably involved in the digestion and the transport of absorbed materials. It is assumed that the collagen fibrils are completely absorbed in the enameloid because no fibrous elements can be found in the proximal cisternae of the ruffled borders. Strong alkaline phosphatase activity has been reported in IDE cells during the maturation stage (Shimoda, 1989). The IDE cells with their ruffled borders that have been observed during enameloid maturation in teleosts should correspond to the ruffle-ended ameloblasts (RA) in mammals. However, these 2 types of cell are different in so far as the IDE cells in teleosts absorb collage fibres (Sasagawa, 1984).

ACKNOWLEDGEMENTS

The author thanks Professor Miles A. Crenshaw, Dental Research Center, University of North Carolina, Chapel Hill, USA for helpful discussions and the staff of Hokuetsu Mizugiken Inc., Niigata for their kindness in offering their facilities for the collection of specimens.

REFERENCES

Garant PR (1970) Observation on the ultrastructure of the ectodermal component during odontogenesis in *Helostoma temmincki*. *Anatomical Record* **166**, 167–188.

Herold RC, Rosenbloom J, Granovsky M (1989) Phylogenetic distribution of enamel proteins: immunohistochemical localization with monoclonal antibodies indicates the evolutionary appearance of enamelins prior to amelogenins. *Calcified Tissue International* **45**, 88–94.

Ishiyama M, Inage T, Shimokawa H, Yoshie S (1994) Immunocytochemical detection of enamel proteins in dental matrix of certain fishes. *Bulletin de l'Institut Océanographique*, *Monaco*, Numéro spécial **14**, 175–182.

Isokawa S, Tsubouchi M, Aoki K, Imai M, Kawai A, Tsuchida S (1970) Studies on the developing enameloid of a fish (*Hoplognathus fasciatus*). I. Mineralization pattern of enameloid matrix. *Journal of the Nihon University School of Dentistry* **12**, 43–49.

Kawasaki K, Fearnhead RW (1983) Comparative histology of tooth enamel and enameloid. In *Mechanisms of Tooth Enamel Formation* (ed. Suga S), pp. 229–238. Tokyo: Quintessence.

Kawasaki K, Shimoda S, Fukae M (1987) Histological and biochemical observations of developing enameloid of the sea bream. *Advances in Dental Research* **1**, 191–195.

Kogaya Y (1989) Histochemical properties of sulfated glycoconjugates in developing enameloid matrix of the fish *Polypterus senegalus*. *Histochemistry* **91**, 185–190.

Kogaya Y (1994) Sulfated glycoconjugates in amelogenesis. In *Progress in Histochemistry and Cytochemistry* (ed. Graumann W), 29, 1–110, Stuttgart: Gustav Fischer.

Linde A, Goldberg M (1993) Dentinogenesis. *Critical Reviews in Oral Biology and Medicine* **4**, 679–728.

Fig. 22. The central to proximal portions of IDE cells (Ide) and distal parts of ODE cells (Ode) that are adjacent to the IDE cells. There are a number of mitochondria, short stretches of rER and a small Golgi apparatus around an elliptical nucleus in the IDE cells. In the ODE cells, extensive labyrinthine canalicular spaces occupy most of the cytoplasm. Demineralised, U-Pb. Bar, 2 μm. Inset: enlarged view of the boundary between the IDE and the ODE cells. An organised arrangement of gap-like junctions and desmosomes is visible. Demineralised. Bar, 500 nm.

Ono T (1974) Electron microscopic studies on the ultrastructure of ameloblasts during amelogenesis in *Oplegnathus fasciatus*. *Japanese Journal of Oral Biology* **16**, 407–464.

Prostak K, Skobe Z (1986) Ultrastructure of the dental epithelium during enameloid mineralization in a teleost fish, *Cichlasoma cyanoguttatum*. *Archives of Oral Biology* **31**, 73–85.

Prostak K, Seifert P, Skobe Z (1991) Tooth matrix formation and mineralization in extant fishes. In *Mechanisms and Phylogeny of Mineralization in Biological Systems* (ed. Suga S, Nakahara H), pp. 465–469. Tokyo: Springer.

Prostak K, Seifert P, Skobe Z (1992) Fish tooth formation: an assessment of biological factors affecting the fluoride content of enameloid. In *Hard Tissue Mineralization and Demineralization* (ed. Suga S, Watabe N), pp. 33–52. Tokyo: Springer.

Prostak K, Seifert P, Skobe Z (1993) Enameloid formation in two tetraodontiform fish species with high and low fluoride contents in enameloid. *Archives of Oral Biology* **38**, 1031–1044.

Sasagawa I (1984) Formation of cap enameloid in the jaw teeth of dog salmon, *Oncorhynchus keta*. *Japanese Journal of Oral Biology* **26**, 477–495.

Sasagawa I (1988) The appearance of matrix vesicles and mineralization during tooth development in three teleost fishes with well-developed enameloid and orthodentine. *Archives of Oral Biology* **33**, 75–86.

Sasagawa I (1992) The accumulation of iron in the dental epithelial cells during enameloid maturation in *Tilapia nilotica*, a teleost. *Japanese Journal of Oral Biology* **34**, 620–624.

Sasagawa I (1993) Iron accumulation in the dental epithelial cells of *Tilapia nilotica*, a teleost. *Archives of Comparative Biology of Tooth Enamel* **3**, 19–28.

Sasagawa I (1995) Fine structure of tooth germs during the formation of enameloid matrix in *Tilapia nilotica*, a teleost fish. *Archives of Oral Biology* **40**, 801–814.

Sasagawa I, Igarashi A (1985) Fine structure of initial calcification during odontogenesis in the dog salmon (*Oncorhynchus keta*, Teleostei). *Japanese Journal of Oral Biology* **27**, 685–698.

Sasagawa I, Ferguson MWJ (1990) Fine structure of the organic matrix remaining in the mature cap enameloid in *Halichoeres poecilopterus*, teleost. *Archives of Oral Biology* **35**, 765–770.

Schmidt WJ (1971) Dentine. In *Polarizing Microscopy of Dental Tissues* (ed. Schmidt WJ, Keil A, trans. Poole DFG, Darling AI), pp. 53–295. Oxford: Pergamon.

Shellis RP, Miles AEW (1974) Autoradiographic study of the formation of enameloid and dentine matrices in teleost fishes using tritiated amino acid. *Proceedings of the Royal Society of London* B **185**, 51–72.

Shellis RP, Miles AEW (1976) Observations with the electron microscope on enameloid formation in common eel (*Anguilla anguilla*; Teleostei). *Proceedings of the Royal Society of London* B **194**, 253–269.

Shimoda S (1989) Histogenesis of sea bream (*Pagrus major*) enameloid. *Tsurumi University Dental Journal* **15**, 267–284.

Ten Cate AR (1989) *Oral Histology*, 3rd edn, pp. 139–156. Toronto: Mosby.

Wakita M (1974) Studies on the ultrastructure of ameloblasts during amelogenesis in *Prionurus microlepidotus* Lacépède. *Japanese Journal of Oral Biology* **16**, 129–185.

Yamashita Y, Ichijo T (1983) Comparative studies on the structure of the ameloblasts. In *Mechanisms of Tooth Enamel Formation* (ed. Suga S), pp. 91–107. Tokyo: Quintessence.